



Preparation of Non-Enzymatic Glucose Sensor Using a Free-Standing Electrode Based on Copper Nanoparticles/Electrospun Carbon Nanofibers Composite

Ali Mohammadpoor¹, Sharareh Sajjadi², Mohsen Rasouli³, Amir Homayoun Keihan^{4*} 

¹ Student Research Committee, Baqiyatallah University of Medical Sciences, Tehran, Iran

² Department of Biology, Roudehen Branch, Islamic Azad University, Roudehen, Iran

³ SEM Lab, Central Laboratory, Amirkabir University of Technology, Tehran, Iran

⁴ Molecular Biology Research Center, Biomedicine Technologies Institute, Baqiyatallah University of Medical Sciences, Tehran, Iran

Corresponding Author: Amir Homayoun Keihan, PhD, Assistant Professor, Molecular Biology Research Center, Biomedicine Technologies Institute, Baqiyatallah University of Medical Sciences, Tehran, Iran. Tel: +98-2187554826, E-mail: ahkyazdan@gmail.com

Received January 6, 2024; Accepted July 8, 2024; Online Published December 30, 2024

Abstract

Introduction: Diabetes mellitus is known as a public health problem worldwide. Accurate detection of glucose concentration is crucial for managing diabetes mellitus. In this study, a non-enzymatic glucose sensor was fabricated using a free-standing electrode based on a composite of copper nanoparticles and electrospun carbon nanofibers.

Materials and Methods: Copper nanoparticles/electrospun carbon nanofibers (Cu/CNFs) nanocomposite was produced using a novel strategy involving electrospinning of polyacrylonitrile/copper acetate (PAN/Cu(OAc)₂), followed by thermal treatment to carbonize the PAN nanofibers and reduce Cu. CuO/CNFs was also synthesized by post-heating the Cu/CNFs nanocomposite. The morphology of the Cu/CNFs nanocomposite was investigated by field emission scanning electron microscopy (FE-SEM), and its composition and structure were characterized by energy-dispersive X-ray (EDX) and X-ray diffraction (XRD) analysis, respectively. The Cu precursor content was optimized by comparing the Raman spectra, conductivity test, and TGA analysis. After demonstrating the effective role of Cu in glucose oxidation, the Cu/CNFs and CuO/CNFs nanocomposites were used directly as free-standing working electrodes for non-enzymatic detection of glucose. The electrochemical responses of the electrodes to glucose were examined by cyclic voltammetry and chronoamperometric techniques.

Results: Compared to the Cu/CNF, the CuO/CNFs showed a higher sensitivity of 424.6 $\mu\text{A mM}^{-1} \text{cm}^{-2}$ and a lower detection limit of 0.35 mM. Both electrodes exhibited a linear range of 2-10 mM.

Conclusions: Reasonable LOD and sensitivity for glucose detection, good selectivity, reasonable stability of one month, and acceptable reproducibility make the CuO/CNFs nanocomposite a promising candidate for the development of non-enzymatic glucose sensors.

Keywords: Copper Nanoparticles, Electrospun Carbon Nanofibers, Non-Enzymatic Sensor, Glucose

Citation: Mohammadpoor A, Sajjadi S, Rasouli M, Keihan AH. Preparation of Non-Enzymatic Glucose Sensor Using a Free-Standing Electrode Based on Copper Nanoparticles/Electrospun Carbon Nanofibers Composite. J Appl Biotechnol Rep. 2024;11(4):1461-1470. doi: [10.30491/jabr.2024.434297.1697](https://doi.org/10.30491/jabr.2024.434297.1697)

Introduction

Diabetes mellitus is known as a public health problem worldwide, characterized by elevated blood glucose levels above the normal range of 3-8 mM. Hyperglycemia occurs due to impaired glucose metabolism resulting from deficiencies in insulin secretion or action.¹ Therefore, accurate detection of glucose concentration is crucial for managing diabetes mellitus.² The development of highly sensitive, reliable, and stable glucose sensors is essential not only for medical diagnosis but also for applications in biotechnology, food, and pharmaceutical industries.^{3,4}

The glucose sensors are commonly categorized into enzymatic and non-enzymatic subgroups.⁵ Enzymatic biosensors, which use the enzyme glucose oxidase (GOx) as the recognition element, demonstrate high sensitivity and selectivity.⁶ However, the high cost and low stability of the

enzyme, along with a complex immobilization process, limit the enzymatic biosensor applications.^{7,8} Additionally, the electrocatalytic properties of GOx could be easily influenced by environmental conditions such as humidity, pH, and temperature.⁹ Therefore, the construction of cost-effective and stable non-enzymatic glucose sensors with high sensitivity has attracted a lot of interest.

Nanostructured materials such as metals (e.g., Pt,¹⁰ Au,¹¹ Ni¹²), transition metal oxides (e.g., CuO,¹³ NiO,¹⁴ Co₃O₄¹⁵), and alloys (e.g., PdNi,¹⁶ PbPt,¹⁷ PtRu¹⁸) are commonly used in the fabrication of non-enzymatic glucose sensors. Among them, copper-based nanoparticles have attracted a lot of attention because of their high electrocatalytic activity and relatively low cost.¹⁹ Carbon-based nanomaterials have been widely used in electrochemical sensors due to their unique

properties such as large specific surface area, high electrical conductivity, excellent mechanical strength, and cost-effectiveness.^{20,21} Carbon nanofibers (CNFs), as one-dimensional carbon-based nanomaterials, have many applications in the construction of electrochemical sensors. They can be effectively used as supports for catalyst nanoparticles.²² Several methods have been developed to grow nanoparticles onto the CNFs surface, including co-precipitation.^{23,24} hydrothermal,^{13,25} and thermal decomposition.^{26,27} Among these methods, the in-situ synthesis of nanoparticle/CNFs nanocomposites from thermal decomposition of precursors has received great attention due to the easy fabrication method and low manufacturing costs. One of the features distinguishing CNFs from other types of carbon-based nanomaterials is that they can be utilized directly as free-standing electrodes without the need for any binder, which increases the conductivity of the electrodes.²⁸ Furthermore, the sensor manufacturing costs will be lower due to the absence of the expensive glassy carbon electrode.

Recently, the electrospinning technique has been known as a simple and cost-effective method for manufacturing CNFs with nanometer diameter and micron length scales.^{29,30} The in-situ process of carbonization of polymer nanofibers and reduction of metallic precursors to metallic nanoparticles can be accomplished by a combination of electrospinning and thermal decomposition processes.¹⁶ So, Cu nanostructures could effectively be prepared and diffuse easily from bulk to the surface of CNFs at high temperatures.³¹ Besides, the size of nanoparticles could be controlled by the temperature and time of the carbonization step and the percentage of salt precursor in the electrospinning solution.³¹

In this work, a novel strategy was used for in-situ growth of Cu (or CuO)/CNFs nanocomposite based on a combination of electrospinning and thermal decomposition methods. The applicability of the proposed nanocomposite as a free-standing electrode for the fabrication of a non-enzymatic glucose sensor was then tested. The prepared nanocomposites were characterized by field emission scanning electron microscopy (FE-SEM), X-ray diffraction (XRD), energy-dispersive X-ray (EDX), Raman spectroscopy, and thermogravimetric analysis (TGA). Electrocatalytic properties of CNFs-based free-standing electrodes (CuO/CNFs and Cu/CNFs) toward the oxidation of glucose were evaluated in alkaline media. The results showed that the prepared electrodes are promising candidates for glucose detection.

Materials and Methods

Synthesis of Cu/CNFs and CuO/CNFs Nanocomposites

In the first step, 1.2 g of polyacrylonitrile (PAN, MW = 80,000 g mol⁻¹, Polyacryle Co.) was dissolved in 10 ml of N, N-dimethylformamide (DMF, Aldrich). After two hours of continuous stirring, different concentrations of copper acetate salt (Cu(Ac)₂.H₂O, Aldrich), i.e. 1, 3, and 5 wt. %, were added

to the above solution and stirred for 24 hours to obtain a homogeneous solution. Next, the electrospinning process was carried out at 11.5 kV to synthesize Cu(Ac)₂/PAN. The feeding rate of the solution was 0.5 ml/h and the needle tip distance from the collector was 10 cm. In the next step, Cu(Ac)₂/PAN nanofibers were stabilized in the air for 1 hour at 230 °C. Cu/CNFs nanocomposites were then prepared by carbonizing the stabilized nanofibers at 900 °C for 2 hours in N₂. The Cu/CNFs nanocomposites containing 1, 3, and 5 wt. % of Cu(Ac)₂.H₂O were designated as 0.1 Cu/CNFs, 0.3 Cu/CNFs, and 0.5 Cu/CNFs, respectively. For higher percentages of copper salt, the viscosity of the electrospinning solution was greatly reduced, and virtually no fibers were obtained on the collector. Therefore, no further efforts were made to obtain nanocomposites with a concentration higher than 5 wt. % of copper salt. Additionally, the carbonized Cu/CNFs were post-heated at 300 °C for 15 minutes in the air to produce CuO/CNFs. The proposed nanocomposite was then used as a free-standing electrode (Supplementary data). The pure CNFs were prepared under the same conditions except that the copper acetate salt was not added.

Characterization of the Nanocomposites

The morphologies of the pure CNFs and Cu/CNFs nanocomposites were characterized by FE-SEM (MIRA3 model, TESCAN Co., Czech Republic). The composition of the Cu/CNFs nanocomposite was investigated by EDX (JEOL, JEM-2010, Japan). The XRD (Microanalyser Unisantix XMF-104, Germany) technique was used to determine the crystal structure of the Cu/CNFs nanocomposite and identify the phase of the samples. Thermo gravimetric analysis (TGA) was conducted in air from 50 to 800 °C. The heating rate was set to be 10 °C min⁻¹. The electrical conductivity of electrodes was determined based on the two-point probe method. The degree of graphitization of the nanocomposites was defined by Raman spectroscopy (Teksan, Takram P50C0R10, Iran), in which the laser wavelength was 532 nm.

Electrochemical Measurements

All electrochemical measurements were conducted using a three-electrode system, with the CNFs, Cu/CNFs, or CuO/CNFs as the working electrode, a platinum plate as the counter electrode, and a saturated Ag/AgCl reference electrode. The measurements were carried out in 0.1 M NaOH at room temperature. Various electrochemical tests, including cyclic voltammetry (CV), chronoamperometry, and electrochemical impedance spectroscopy (EIS), were performed using a Potentiostat/Galvanostat (Autolab PGSTAT 204N, Netherlands). The CV measurements were conducted in the potential range of 0.2-0.8 V at a scan rate of 50 mV s⁻¹. EIS (10⁻² to 10⁵ Hz with an AC amplitude of 5 mV) was performed in a 0.1 M KCl electrolyte solution containing 5 mM [Fe(CN)₆]^{3-/4-}.

Results and Discussion

Morphological Structure and Composition

Figures 1A and B show the FE-SEM images of the pure CNFs and Cu/CNFs nanocomposite. As seen, the pure CNFs showed a fibrillar morphology with fiber-fiber interconnections. Compared with the pure CNFs, the Cu/CNFs nanocomposite showed a more uniform morphology with no interconnections. Also, the diameter of the Cu/CNFs nanocomposite was calculated by Image J software, varying from 220-400 nm. Thus, the fiber diameter increased in the Cu/CNFs compared with that of the pure CNFs (Figure 1B). Additionally, according to Figure 1B, the Cu nanoparticles were almost uniformly dispersed on the CNFs surface. The size of the Cu nanoparticles on the CNFs surface, measured by Image J software (Figure 1C), ranged from 250 to 550 nm, with an average size of 387.5 nm. To achieve the uniform dispersion of Cu nanoparticles, the temperature and time of the carbonization step were tested in the range of 700-1000 °C and 1-5 hours, respectively. The optimum temperature and time of the carbonization process were determined to be

900 °C and 2 hours, respectively.

The composition and crystal structure of the Cu/CNFs nanocomposite were studied using EDX and XRD techniques. According to Figure 1D, the EDX spectrum of the Cu/CNFs nanocomposite showed peaks assigning to the C, N, O, and Cu elements, confirming the successful formation of the Cu/CNFs nanocomposite. The quantitative composition analysis revealed that the Cu/CNFs consisted of 53.28 wt. % C, 21.24 wt. % Cu, 7.93 wt. % O, and 17.55 wt. % N. The peak of N may be attributed to the remaining nitrogen atoms on the CNFs surface as a result of using PAN as a precursor.

The crystal structure of the Cu/CNFs nanocomposite was studied by XRD (Figure 1E). The XRD of the Cu/CNFs showed a diffraction peak at $2\theta = 24^\circ\text{-}26^\circ$, attributed to the graphitized basal planes (002).^{32,33} Additionally, three diffraction peaks at $2\theta = 43.5^\circ$, 50.5° , and 74.5° were observed, corresponding to the diffraction peaks of (111), (200), and (220) planes in the face-centered cubic Cu crystal structure, respectively.³⁴ The XRD results further confirmed the presence of copper and carbon in the Cu/CNFs nanocomposite.

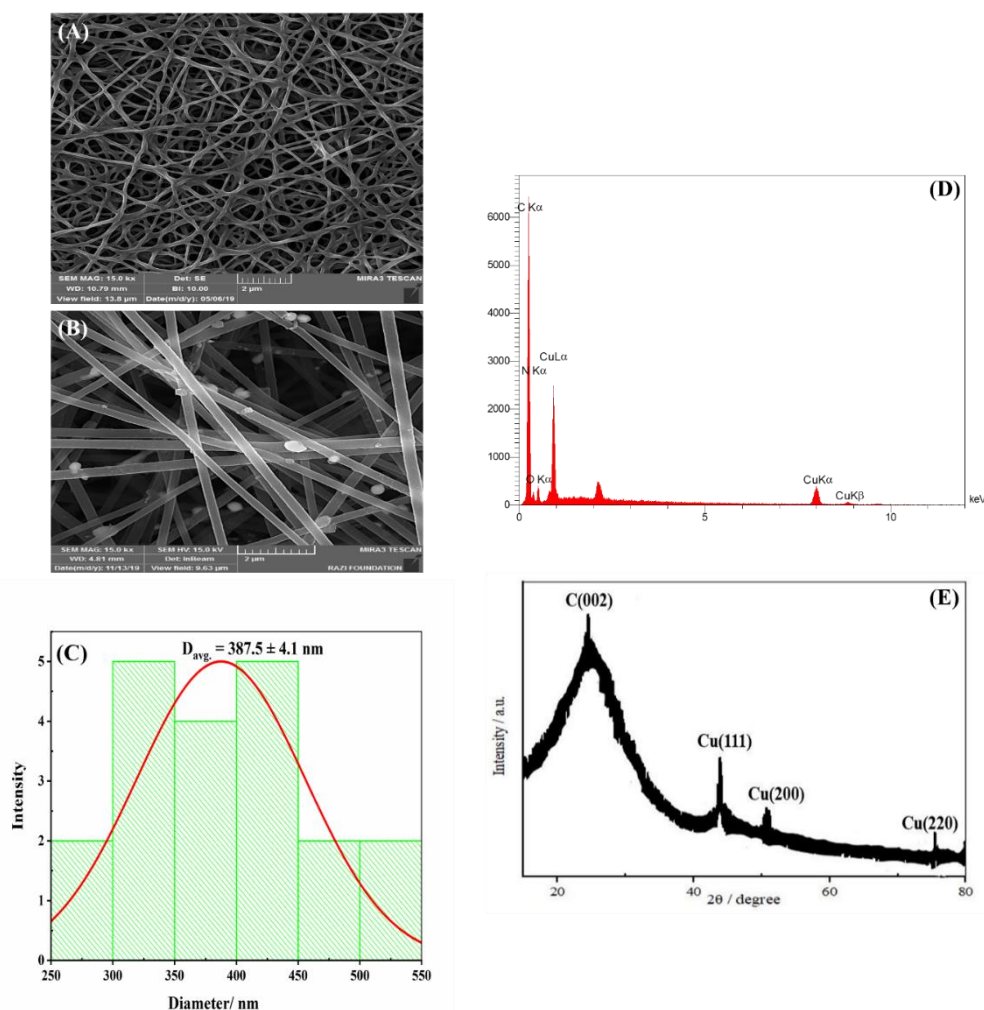


Figure 1. Characterization of Nanocomposite. (A) and (B) FE-SEM images of pure CNFs and Cu/CNFs nanocomposite, respectively; (C) histogram of Cu/CNF; (D) EDX of the Cu/CNFs nanocomposite, and (E) XRD pattern of the Cu/CNFs nanocomposite.

Optimization of the Metal Precursor

Raman Spectroscopy

Raman spectroscopy was used to investigate the effect of the metal precursor content on the structure of the Cu/CNFs nanocomposite. Figure 2A shows the Raman spectra of the Cu/CNFs nanocomposites with different metal precursor contents. As seen, all of the nanocomposites showed two characteristic peaks at ~ 1350 and 1580 cm^{-1} that could be attributed to the D-band and G-band, respectively. The D-band corresponds to the structural disorder, arising from defects, and the G-band is assigned to the stretching vibrations

of sp^2 carbon atoms in graphite layers.^{36,37} The R-values (D-band/G-band intensity ratio) for the three nanocomposites are shown in Table 1. By increasing the metal precursor contents in the Cu/CNF nanocomposites from 1 to 5 wt. %, the R-value decreased from 1.063 to 0.942. A lower R-value depicted a higher degree of graphitization and higher sp^2 content for carbon materials. Also, for higher percentages of copper salt, the viscosity of the electrospinning solution was greatly reduced, and virtually no fibers were obtained on the collector. Therefore, the 0.5 Cu/CNFs nanocomposite exhibited the highest degree of graphitization (Table 1).

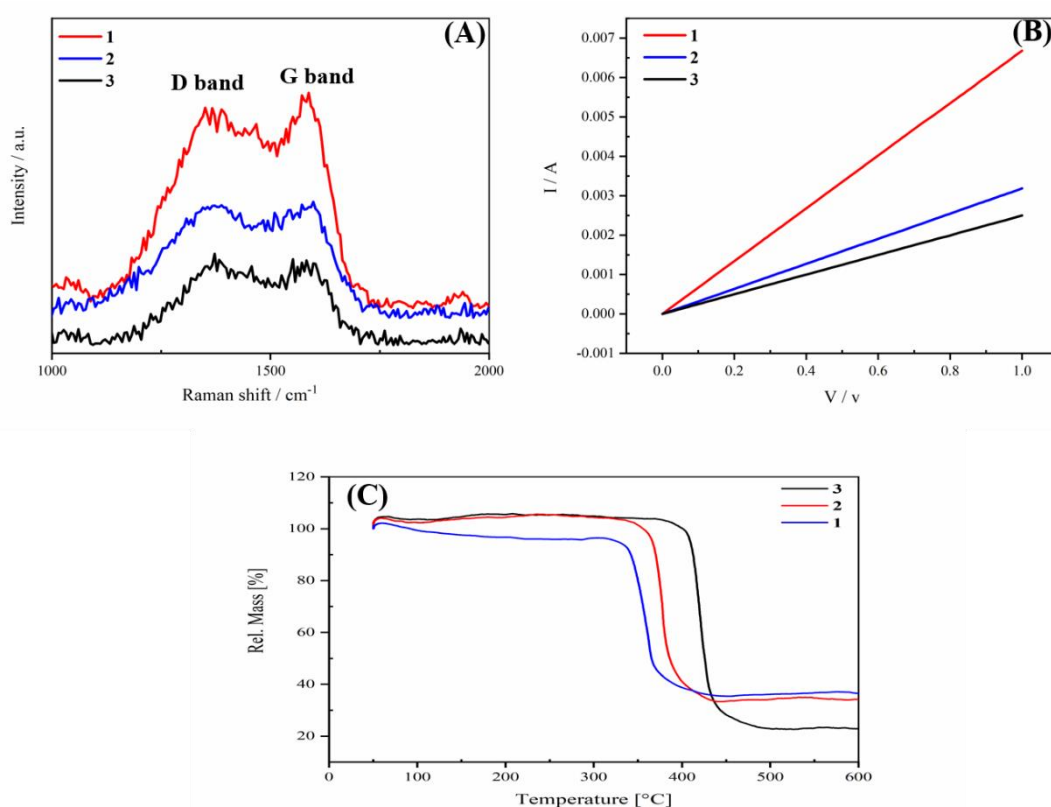


Figure 2. Characterization of Nanocomposites by (A) Raman spectra, (B) Electrical conductivity, and (C) TGA curves of Cu/CNFs nanocomposites for 1) 0.5 Cu/CNFs, 2) 0.3 Cu/CNFs, and 3) 0.1 Cu/CNFs. The electrical conductivity measurement was done for 5 times under the same conditions and the average I-V curve is shown.

Table 1. R value, Degree of Graphitization, Conductance, Thickness, and Electrical Conductivities of Cu/CNFs Nanocomposites Containing Different Amounts of $\text{Cu}(\text{OAc})_2$ Precursor

Samples	R value $= \frac{I_D}{I_G}$	Degree of graphitization $= \frac{I_G}{I_D + I_G} \times 100$	Conductance $= 1/R$ (S)	Thickness of samples (μm)	Electrical conductivity (S/cm) $\sigma = \frac{1}{R} \times \frac{L}{A}$
0.1 Cu/CNFs	1.063	48.46	0.0025	30	0.83
0.3 Cu/CNFs	0.970	50.73	0.0032	25	1.28
0.5 Cu/CNFs	0.942	51.49	0.0066	45	1.46

Electrical Conductivity

The two-probe Keithley instrument was used to measure the I-V curve of the Cu/CNFs nanocomposite. Figure 2B shows the electrical conductivity of the 0.1, 0.3, and 0.5 Cu/CNFs nanocomposites in the voltage range of 0-1 V.

The electrical conductivity of the Cu/CNFs nanocomposites is compared in Table 1. As seen, the highest electrical conductivity was obtained for the 0.5 Cu/CNFs nanocomposite, which contained the largest amount of Cu. The electrical conductivity data confirmed the Raman spectroscopy results,

in which the highest degree of graphitization was observed in the 0.5 Cu/CNF nanocomposite. Thus, the 0.5 Cu/CNFs was selected as the optimal sample and was calcinated in an air furnace at 300 °C for 15 minutes in order to achieve the precipitation of the CuO/CNFs.

TGA Analysis

To investigate the thermal stability of the nanocomposites, TGA analysis was performed at 25-600 °C under an air atmosphere. According to Figure 2C, the 0.1, 0.3, and 0.5 Cu/CNF nanocomposites demonstrated significant weight loss at ~350, 375, and 400 °C, respectively. The weight loss occurred as a result of the oxidation of the CNFs. It is noteworthy that the weight loss in the 0.5 Cu/CNF sample initiated earlier due to the higher percentage of copper in the nanocomposite and its higher thermal conductivity. The remaining weight percentage at 600 °C belongs to the copper metal, which is obtained as 23.32, 34.28, and 37.11 for 0.1, 0.3, and 0.5 Cu/CNF nanocomposites, respectively.

Electrochemical and Electrocatalytic Properties of the Electrodes

The electrochemical properties of the pure CNFs and

Cu/CNFs nanocomposite were studied by CV experiments in a 0.1 M NaOH alkaline solution at a scan rate of 50 mV s⁻¹. In all electrochemical experiments, the CNFs or Cu/CNFs nanocomposite was used as a free-standing electrode. According to Figure 3A (black line), it is obvious that the pure CNFs showed no redox peak, while for Cu/CNFs (Figure 3B, black line), a cathodic peak at ~0.3 and an anodic peak at ~0.5 were observed, which could be attributed to the electrocatalytic activity of the Cu²⁺/Cu³⁺ redox pairs in the alkaline medium.³

To study the electrocatalytic properties of the pure CNFs and Cu/CNFs nanocomposites towards glucose oxidation, CV analysis was also performed in the presence of 4 mM glucose. As seen, the addition of glucose made no considerable change to the CV curve of the pure CNFs (Figure 3A, red line). Therefore, the pure CNFs were not capable of catalyzing glucose. However, for the Cu/CNFs nanocomposite, the anodic peak current increased in the presence of glucose (Figure 3B, red line), indicating the high ability of the copper nanoparticles to catalyze glucose oxidation. The oxidation of glucose at 0.55 V is accompanied by the conversion of Cu²⁺/Cu³⁺.³⁸ It has been suggested that Cu³⁺ species act as an electron transfer mediator for glucose oxidation.³⁹

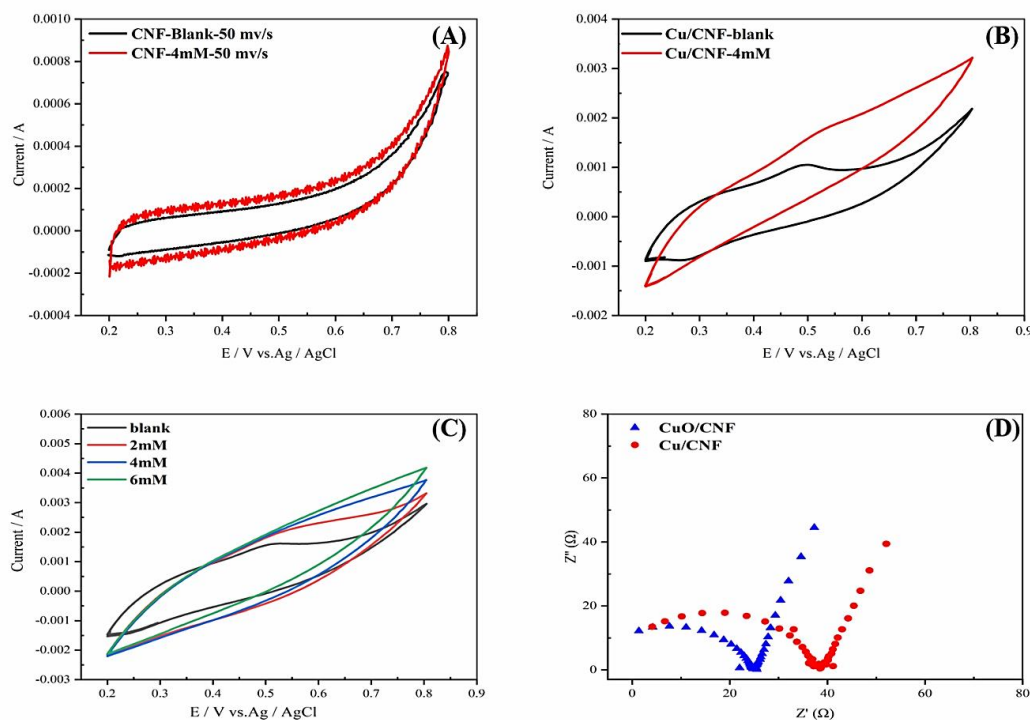


Figure 3. Electrochemical and Electrocatalytic Properties of the Electrodes. CVs of (A) CNFs and (B) Cu/CNFs nanocomposite in 0.1 M NaOH solution in the absence (black line) and presence (red line) of 4 mM glucose; (C) The effect of glucose concentration on the anodic peak current of Cu/CNFs electrode in 0.1 M NaOH solution at a scan rate of 50 mV s⁻¹; (D) EIS of CuO/CNFs (blue) and Cu/CNFs (red) electrodes in 0.1 M KCl electrolyte solution containing 5 mM [Fe(CN)₆]^{3-/4-}.

Figure 3C illustrates the effect of glucose concentration on the Cu/CNFs electrode's current response. It was observed that the anodic peak current increased by increasing the

concentration of glucose, which indicates the ability of the electrode to measure the glucose concentration.

After verifying the catalyzing role of copper in glucose

oxidation, a one-stage post-heating was carried out on the Cu/CNFs nanocomposites in order to compare the electrocatalytic properties of Cu/CNFs and CuO/CNFs using EIS experiments. Figure 3D shows the Nyquist plot of Cu/CNFs and CuO/CNFs nanocomposites in the frequency range of 0.1 Hz to 100 kHz. The straight line at lower frequencies denotes the Warburg impedance, indicating a diffusion-controlled process. In the high-frequency region, the data were fitted to a Randles equivalent circuit, and the values of charge transfer resistance (R_{ct}) for Cu/CNFs and CuO/CNFs electrodes were obtained as 39 and 31 Ω , respectively. The lower charge transfer resistance in CuO/CNFs could make the electron transfer kinetics process easier.⁴⁰ This demonstrates that the CuO/CNFs electrode

had higher electrical conductivity compared to the Cu/CNFs electrode.

Analytical Characteristics of the Sensor

The calibration curve for glucose determination was obtained based on the chronoamperometric response to the successive injection of 0.5 M glucose in 0.1 M NaOH solution. Initially, to determine the appropriate applied potential, chronoamperometric measurements were conducted at various potentials ranging from 0.3 to 0.6 V. As depicted in Figure 4, the current response increased with an increase in potential up to 0.55 V. Further elevation of the potential led to a decrease in the amperometric response. Therefore, 0.55 V was selected as the optimal potential.

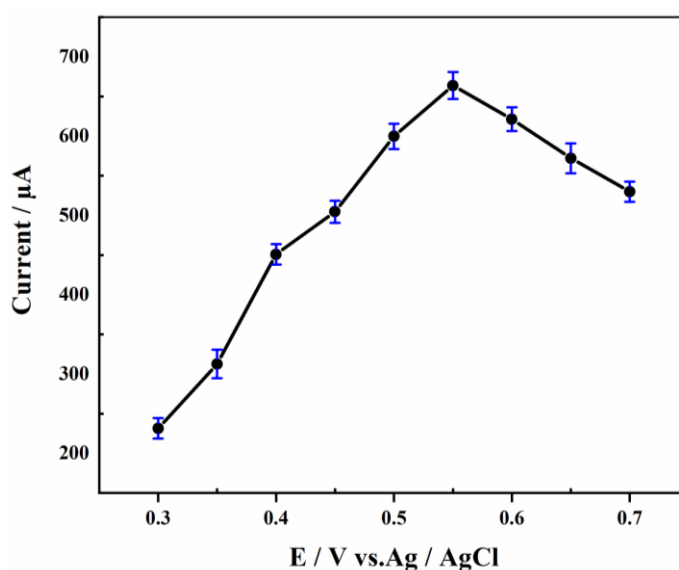


Figure 4. The Calibration Curve for Glucose Determination. The effect of applied potential on the amperometric response of the sensor to 2.0 mM glucose in 0.10 M NaOH.

Figure 5A shows the amperometric responses of the Cu/CNFs and CuO/CNFs electrodes to successive additions of 0.5 mM glucose into 0.1 M NaOH solution at an applied potential of +0.55 V. The resulting calibration curves of the Cu/CNFs and CuO/CNFs electrodes are shown in Figure 5B, and the electroanalytical parameters of both electrodes are summarized in Table 2. Both electrodes exhibited the same linear range (2-10 mM), which could successfully measure normal physiological blood glucose levels (3-8 mM).⁴¹ The sensitivity, calculated from the slope of the linear part of the calibration curve, was found to be 301.15 and 426.60 $\mu\text{A mM}^{-1} \text{cm}^{-2}$ for Cu/CNFs and CuO/CNFs electrodes, respectively. The higher sensitivity of the CuO/CNFs electrode could be attributed to the better electrocatalytic properties of copper oxide, which has a higher ability to oxidize glucose.⁴¹ Additionally, CuO promotes the $\text{Cu}^{2+}/\text{Cu}^{3+}$ transformation. The resulting Cu^{3+} ions are considered to be the main species necessary for the oxidation of glucose on the copper-based

electrodes in alkaline media (reaction 1)⁴²:



The high performance of the CuO/CNFs electrode may be attributed to higher electrical conductivity compared to the Cu/CNFs electrode, as demonstrated by impedance analysis (Figure 3D). The limit of detection (LOD) was determined using the equation $\text{LOD} = 3.3 \sigma / S$, where σ is the standard deviation of the blank (0.1 M NaOH solution) and S is the slope of the calibration curve. The LOD for glucose detection was calculated to be 0.90 mM and 0.35 mM for the Cu/CNFs and CuO/CNFs electrodes, respectively. Since the CuO/CNFs electrode exhibited superior analytical parameters compared to the Cu/CNFs electrode, it was selected for further experiments.

Table 3 shows a comparison between the analytical characteristics of the proposed sensor and some other non-

enzymatic glucose sensors. It can be observed that, compared with other glucose sensors, the detection limit and linear range of the proposed sensor were reasonable.

Although some other non-enzymatic glucose sensors could detect lower amounts of glucose, the proposed sensor exhibited higher sensitivity.

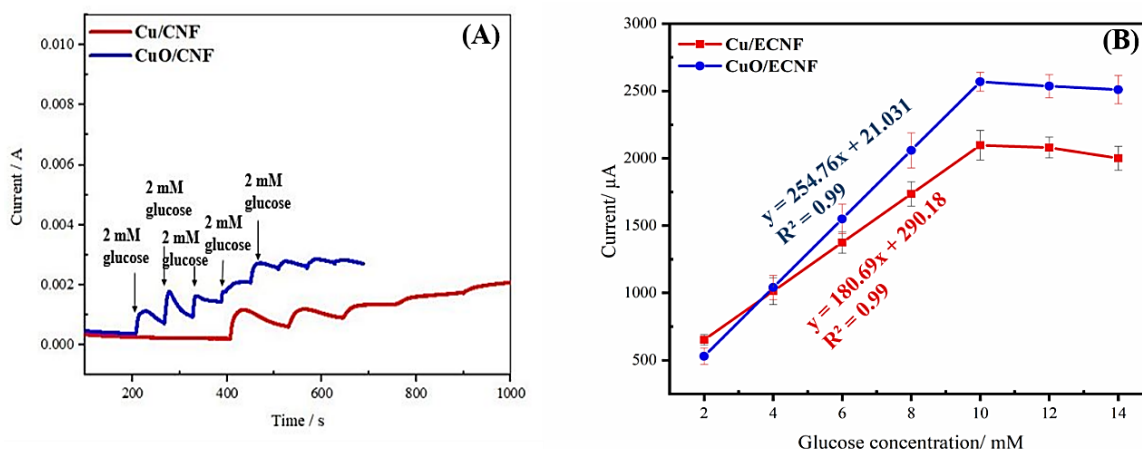


Figure 5. Amperometric Responses of the Cu/CNFs and CuO/CNFs Electrodes to Glucose. (A) Amperometric response of Cu/CNFs (red line) and CuO/CNFs (blue line) electrodes at +0.55V upon successive addition of 0.5 M glucose to 0.1 M NaOH solution; (B) The calibration curves of the Cu/CNFs and CuO/CNFs electrodes for glucose detection.

Table 2. Comparison of the Electroanalytical Parameters of Cu/CNFs and CuO/CNFs Electrodes for Glucose Detection

Sample name	Sensitivity ($\mu\text{A mM}^{-1} \text{cm}^{-2}$)	Linear range (mM)	LOD (mM)
Cu/CNFs	301.15	2-10	0.90
CuO/CNFs	424.60	2-10	0.35

Table 3. Comparison of Analytical Performance of the Present Sensors with other Nonenzymatic Glucose Sensors

Electrode	Sensitivity ($\mu\text{A} \cdot \text{mM}^{-1} \cdot \text{cm}^{-2}$)	Linear range (mM)	LOD (mM)	References
Cu NPs/SWCNT ^a /Nafion	256	-	25×10^{-5}	(43)
CuO nanowires	0.49	4×10^{-4} -2	49×10^{-6}	(44)
Cu/graphene	-	Up to 4.5	5×10^{-4}	(8)
Cu ₂ O/MWCNTs ^b GCE	92.4	Up to 0.01	5×10^{-5}	(45)
Cu NBS ^c	79.8	-	0.01	(38)
CuNPs	246	0.001-0.17	-	(46)
GCE/MWCNT/Cu oxy-hydroxide nanoparticle	51.1	0.2-5	0.33	(47)
Pt-replaced porous Cu frameworks	9.62	1-11	0.385	(48)
AuCu@ Cu-10	8.52	1-5	0.43	(49)
Cu/CNFs	301.15	2-10	0.9	This work
CuO/CNFs	424.6	2-10	0.35	This work

^a single-walled carbon nanotube; ^b multi-walled carbon nanotubes; ^c nanobelts.

Selectivity, Reproducibility and Stability of the Sensor

There are other species in the real blood sample that may interfere with glucose detection. So, the selectivity of the proposed sensor was tested in the presence of ascorbic acid (AA), uric acid (UA), and dopamine (DA). The normal concentration of glucose in the blood is in the range of 3-8 mM, while the level of interfering species is nearly 0.1 mM.⁵⁰ Therefore, the electrode’s chronoamperometric test was evaluated at +0.55 V by alternate addition of 4 mM glucose, 0.1 mM of AA, UA and DA and 2 mM glucose to 0.1 M NaOH solution. As seen in Figure 6, no significant response currents were observed for these interfering species, indicating that the proposed sensor had a good selectivity for detecting glucose.

To investigate the storage stability of the sensor, after three weeks of soaking in 0.1 M NaOH solution, three electrodes were taken again for a CV test. There was no difference between the results from the previous electrodes and these electrodes. Consequently, the electrodes had good stability. To assess the operational stability of the sensor, the prepared electrodes were stored in the air (at room temperature), and the amperometric response of the sensor to 4 mM glucose was measured during one month. The results showed that the current response preserved about 95% of its initial value after one month, showing the reasonable stability of the sensor.

The reproducibility of the proposed sensor was tested by comparing the amperometric current response of three

different CuO/CNFs electrodes, made with the same method, to 2 mM glucose in 0.1 M NaOH. The relative standard

deviation (RSD) was obtained as ~3.5%, showing an acceptable reproducibility of the sensor.

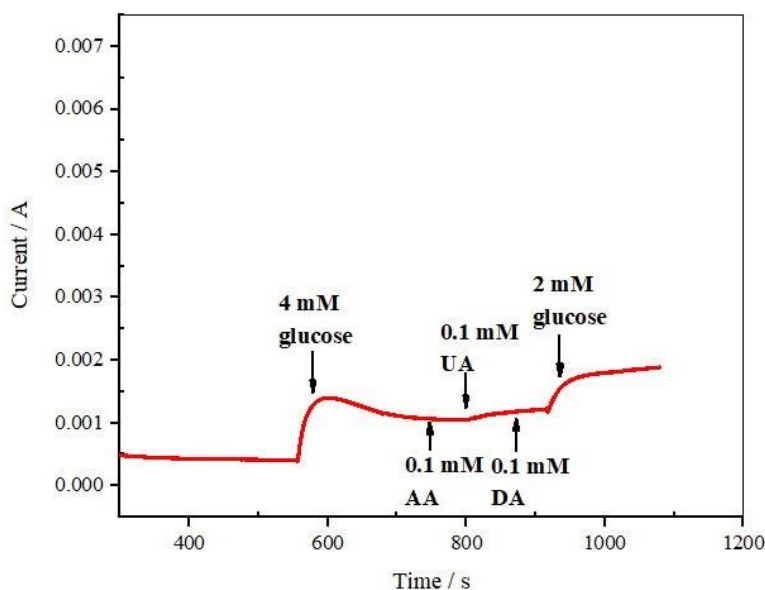


Figure 6. Selectivity of the Sensor. The amperometric response of the biosensor to injections of 4.0- and 2.0-mM glucose and 0.10 mM interferents of AA, UA, and DA in a 0.10 M NaOH solution.

Conclusion

In brief, a uniform dispersion of copper-based nanoparticles (Cu and CuO) on the surface of CNFs was obtained by a combination of the electrospinning method and heat treatment. The morphology and microstructure of the nanocomposites were characterized by FE-SEM, EDX, and XRD. The Cu precursor content was optimized by comparing the Raman spectra, conductivity test, and TGA analysis. Then, the resulting nanocomposites were directly employed in the form of free-standing electrodes for constructing non-enzymatic glucose sensors without the need for a binder. The CV experiments showed that Cu was able to oxidize glucose. In the next step, the Cu/CNFs and CuO/CNFs electrodes were compared in terms of charge transfer resistance and electroanalytical parameters for glucose detection. The results showed that the CuO/CNF electrode demonstrated lower charge transfer resistance and better analytical parameters. The proposed non-enzymatic sensor showed good selectivity, acceptable repeatability, and high stability, making it a promising candidate for practical applications.

Authors' Contributions

All authors contributed to the conception and design of the study, wrote the first draft of the manuscript, manuscript revision, and approved the submitted version.

Conflict of Interest Disclosures

The authors declare that they have no conflicts of interest.

Acknowledgment

The authors appreciate the SEM Lab of the Central Laboratory of Amirkabir University of Technology, Tehran, Iran.

References

- Mukhtar Y, Galalain A, Yunusa U. A modern overview on diabetes mellitus: a chronic endocrine disorder. *Eur J Biol.* 2020;5(2):1-14. doi:10.47672/ejb.409
- Teymourian H, Barfidokht A, Wang J. Electrochemical glucose sensors in diabetes management: an updated review (2010–2020). *Chem Soc Rev.* 2020;49(21):7671-709. doi:10.1039/D0CS00304B
- Chadha U, Bhardwaj P, Agarwal R, Rawat P, Agarwal R, Gupta I, et al. Recent progress and growth in biosensors technology: A critical review. *J Ind Eng Chem.* 2022;109:21-51. doi:10.1016/j.jiec.2022.02.010
- Mahheidari N, Rashidiani J, Akbariqomi M, Eskandari K, Banaei A. Novel Glucose Biosensor Based on Citrullus Colocynthis and Urtica Dioica. *Curr Biotechnol.* 2023;12(1):37-44. doi.org/10.2174/2211550112666221219095851
- Zhu H, Li L, Zhou W, Shao Z, Chen X. Advances in non-enzymatic glucose sensors based on metal oxides. *J Mater Chem B.* 2016;4(46):7333-49. doi:10.1039/C6TB02037B
- Mani V, Devadas B, Chen SM. Direct electrochemistry of glucose oxidase at electrochemically reduced graphene oxide-multiwalled carbon nanotubes hybrid material modified electrode for glucose biosensor. *Biosens Bioelectron.* 2013;41:309-15. doi:10.1016/j.bios.2012.08.045
- Si P, Huang Y, Wang T, Ma J. Nanomaterials for electrochemical non-enzymatic glucose biosensors. *RSC Adv.* 2013;3(11):3487-502. doi:10.1039/C2RA22360K
- Luo J, Jiang S, Zhang H, Jiang J, Liu X. A novel non-enzymatic glucose sensor based on Cu nanoparticle

- modified graphene sheets electrode. *Anal Chim Acta*. 2012;709:47-53. doi:10.1016/j.aca.2011.10.025
9. Kumar R, Singh L. Ti3C2Tx MXene as electrocatalyst for designing robust glucose biosensors. *Adv Mater Technol*. 2022;7(12):2200151. doi:10.1002/admt.202200151
10. Gu S, Lu Y, Ding Y, Li L, Song H, Wang J, Wu Q. A droplet-based microfluidic electrochemical sensor using platinum-black microelectrode and its application in high sensitive glucose sensing. *Biosens Bioelectron*. 2014;55:106-12. doi:10.1016/j.bios.2013.12.002
11. Chen M, Cao X, Chang K, Xiang H, Wang R. A novel electrochemical non-enzymatic glucose sensor based on Au nanoparticle-modified indium tin oxide electrode and boronate affinity. *Electrochimica Acta*. 2021;368:137603. doi:10.1002/elan.201400347
12. Fall B, Sall DD, Hémadi M, Diaw AK, Fall M, Randriamahazaka H, et al. Highly efficient non-enzymatic electrochemical glucose sensor based on carbon nanotubes functionalized by molybdenum disulfide and decorated with nickel nanoparticles (GCE/CNT/MoS2/NiNPs). *Sens Actuators Rep*. 2023;5:100136. doi:10.1016/j.snr.2022.100136
13. Lu N, Shao C, Li X, Miao F, Wang K, Liu Y. CuO nanoparticles/nitrogen-doped carbon nanofibers modified glassy carbon electrodes for non-enzymatic glucose sensors with improved sensitivity. *Ceram Int*. 2016;42(9):11285-93. doi:10.1016/j.ceramint.2016.04.046
14. Youcef M, Hamza B, Nora H, Walid B, Salima M, Ahmed B, et al. A novel green synthesized NiO nanoparticles modified glassy carbon electrode for non-enzymatic glucose sensing. *Microchem J*. 2022;178:107332. doi:10.1016/j.microc.2022.107332
15. Xiong LY, Kim YJ, Seo WC, Lee HK, Yang WC, Xie WF. High-performance non-enzymatic glucose sensor based on Co3O4/rGO nanohybrid. *Rare Metals*. 2023;42(9):3046-53. doi:10.1007/s12598-023-02318-9
16. Guo Q, Liu D, Zhang X, Li L, Hou H, Niwa O, et al. Pd-Ni alloy nanoparticle/carbon nanofiber composites: preparation, structure, and superior electrocatalytic properties for sugar analysis. *Anal Chem*. 2014;86(12):5898-905. doi:10.1021/ac500811j
17. Cui HF, Ye JS, Zhang WD, Li CM, Luong JH, Sheu FS. Selective and sensitive electrochemical detection of glucose in neutral solution using platinum-lead alloy nanoparticle/carbon nanotube nanocomposites. *Anal Chim Acta*. 2007;594(2):175-83. doi:10.1016/j.aca.2007.05.047
18. Li LH, Zhang WD, Ye JS. Electrocatalytic oxidation of glucose at carbon nanotubes supported PtRu nanoparticles and its detection. *Electroanalysis*. 2008;20(20):2212-6. doi:10.1002/elan.200804312
19. Li K, Xu X, Liu W, Yang S, Huang L, Tang S, et al. A copper-based biosensor for dual-mode glucose detection. *Front Chem*. 2022;10:861353. doi:10.3389/fchem.2022.861353
20. Goldoni A, Alijani V, Sangaletti L, D'Arsiè L. Advanced promising routes of carbon/metal oxides hybrids in sensors: A review. *Electrochimica Acta*. 2018;266:139-50. doi:10.1016/j.electacta.2018.01.170
21. Baptista FR, Belhout SA, Giordani S, Quinn SJ. Recent developments in carbon nanomaterial sensors. *Chem Soc Revs*. 2015;44(13):4433-53. doi:10.1039/C4CS00379A
22. Liu Y, Wang D, Huang J, Hou H, You T. Highly sensitive composite electrode based on electrospun carbon nanofibers and ionic liquid. *Electrochem Commun*. 2010;12(8):1108-11. doi:10.1016/j.elecom.2010.05.041
23. Al-Enizi AM, Ghanem MA, El-Zatahry AA, Al-Deyab SS. Nickel oxide/nitrogen doped carbon nanofibers catalyst for methanol oxidation in alkaline media. *Electrochimica Acta*. 2014;137:774-80. doi:10.1016/j.electacta.2014.05.150
24. Zhang J, Zhu X, Dong H, Zhang X, Wang W, Chen Z. In situ growth cupric oxide nanoparticles on carbon nanofibers for sensitive nonenzymatic sensing of glucose. *Electrochimica Acta*. 2013;105:433-8. doi:10.1016/j.electacta.2013.04.169
25. Liu L, Wang Z, Yang J, Liu G, Li J, Guo L, et al. NiCo2O4 nanoneedle-decorated electrospun carbon nanofiber nanohybrids for sensitive non-enzymatic glucose sensors. *Sens Actuators B: Chem*. 2018;258:920-8. doi:10.1016/j.snb.2017.11.118
26. Huang J, Zhang B, Xie YY, Lye WW, Xu ZL, Abouali S, et al. Electrospun graphitic carbon nanofibers with in-situ encapsulated Co-Ni nanoparticles as freestanding electrodes for Li-O2 batteries. *Carbon*. 2016;100:329-36. doi:10.1016/j.carbon.2016.01.012
27. Liu D, Guo Q, Zhang X, Hou H, You T. PdCo alloy nanoparticle-embedded carbon nanofiber for ultrasensitive nonenzymatic detection of hydrogen peroxide and nitrite. *J Colloid Interface Sci*. 2015;450:168-73. doi:10.1016/j.jcis.2015.03.014
28. Mohammadpour-Haratbar A, Mohammadpour-Haratbar S, Zare Y, Rhee KY, Park SJ. A review on non-enzymatic electrochemical biosensors of glucose using carbon nanofiber nanocomposites. *Biosensors*. 2022;12(11):1004. doi:10.3390/bios12111004
29. Svinterikos E, Zuburtikudis I, Al-Marzouqi M. Electrospun lignin-derived carbon micro-and nanofibers: A review on precursors, properties, and applications. *ACS Sustain Chem Eng*. 2020;8(37):13868-93. doi:10.1021/acsuschemeng.0c03246
30. Lee BS, Yu WR. Electrospun carbon nanofibers as a functional composite platform: A review of highly tunable microstructures and morphologies for versatile applications. *Funct Compos Struct*. 2020;2(1):012001. doi:10.1088/2631-6331/ab7a8c
31. Mohammadpour-Haratbar A, Mosallanejad B, Zare Y, Rhee KY, Park SJ. Co3O4 nanoparticles embedded in electrospun carbon nanofibers as free-standing nanocomposite electrodes as highly sensitive enzyme-free glucose biosensors. *Rev Adv Mater*. 2022;61(1):744-55. doi:10.1515/rams-2022-0251
32. Ali H, Verma N. A Cu-CNF-rGO-functionalized carbon film indicated as a versatile electrode for sensing of biomarkers using electropolymerized recognition elements. *J Mater Sci*. 2022;57(11):6345-60. doi:10.1007/s10853-022-07029-7
33. Li G, Yuan H, Mou J, Dai E, Zhang H, Li Z, et al. Electrochemical detection of nitrate with carbon nanofibers and copper co-modified carbon fiber electrodes. *Compos Commun*. 2022;29:101043. doi:10.1016/j.coco.2021.10.1043
34. Zhao Y, Liu Y, Zhang Z, Mo Z, Wang C, Gao S. Flower-like open-structured polycrystalline copper with synergistic multi-crystal plane for efficient electrocatalytic reduction of nitrate to ammonia. *Nano Energy*. 2022;97:107124. doi:10.1016/j.nanoen.2022.107124
35. Puchý V, Tatarko P, Dusza J, Morgiel J, Bastl Z, Mihály J. Characterization of carbon nanofibers by SEM, TEM, ESCA and Raman spectroscopy. *Kovove Mater*. 2010;48(6):379-85. doi:10.4149/km.2010.6.379
36. De Oliveira JB, Guerrini LM, Oishi SS, de Oliveira Hein LR, dos Santos Conejo L, Rezende MC, et al. Carbon nanofibers obtained from electrospinning process. *Mater Res Express*. 2018;5(2):025602. doi:10.1088/2053-1591/aaa467
37. Luo P, Prabhu SV, Baldwin RP. Constant potential amperometric detection at a copper-based electrode:

- electrode formation and operation. *Anal Chem.* 1990; 62(7):752-5. doi:10.1021/ac00206a021
38. Huang TK, Lin KW, Tung SP, Cheng TM, Chang IC, Hsieh YZ, et al. Glucose sensing by electrochemically grown copper nanobelt electrode. *J Electroanal Chem.* 2009;636(1-2):123-7. doi:10.1016/j.jelechem.2009.08.011
39. Wang J, Chen G, Wang M, Chatrathi MP. Carbon-nanotube/copper composite electrodes for capillary electrophoresis microchip detection of carbohydrates. *Analyst.* 2004;129(6):512-5. doi:10.1039/B401503G
40. Ren X, Pickup PG. An impedance study of electron transport and electron transfer in composite polypyrrole+ polystyrenesulphonate films. *J Electroanal Chem.* 1997; 420(1-2):251-7. doi:10.1016/S0022-0728(96)04784-5
41. Ahmad R, Khan M, Mishra P, Jahan N, Ahsan MA, Ahmad I, et al. Engineered hierarchical CuO nanoleaves based electrochemical nonenzymatic biosensor for glucose detection. *J Electrochem Soc.* 2021;168(1): 017501. doi:10.1149/1945-7111/abd515
42. Hassan HB, Hamid ZA. Electrodeposited Cu–CuO composite films for electrochemical detection of glucose. *Int J Electrochem Sci.* 2011;6(11):5741-58. doi:10.1016/S1452-3981(23)18441-0
43. Zhang Y, Su L, Manuzzi D, de los Monteros HV, Jia W, Huo D, et al. Ultrasensitive and selective non-enzymatic glucose detection using copper nanowires. *Biosens Bioelectron.* 2012;31(1):426-32. doi:10.1016/j.bios.2011.11.006
44. Zhuang Z, Su X, Yuan H, Sun Q, Xiao D, Choi MM. An improved sensitivity non-enzymatic glucose sensor based on a CuO nanowire modified Cu electrode. *Analyst.* 2008;133(1):126-32. doi:10.1039/B712970J
45. Zhang X, Wang G, Zhang W, Wei Y, Fang B. Fixure-reduce method for the synthesis of Cu₂O/MWCNTs nanocomposites and its application as enzyme-free glucose sensor. *Biosens Bioelectron.* 2009;24(11):3395-8. doi:10.1016/j.bios.2009.04.031
46. Li Y, Wei Y, Shi G, Xian Y, Jin L. Facile synthesis of leaf-like CuO nanoparticles and their application on glucose biosensor. *Electroanalysis.* 2011;23(2):497-502. doi:10.1002/elan.201000343
47. De Sá AC, Cipri A, González-Calabuig A, Stradiotto NR, Del Valle M. Resolution of galactose, glucose, xylose and mannose in sugarcane bagasse employing a voltammetric electronic tongue formed by metals oxy-hydroxide/MWCNT modified electrodes. *Sens Actuators B: Chem.* 2016;222:645-53. doi:10.1016/j.snb.2015.08.088
48. Hu Y, Niu X, Zhao H, Tang J, Lan M. Enzyme-free amperometric detection of glucose on platinum-replaced porous copper frameworks. *Electrochimica Acta.* 2015; 165:383-9. doi:10.1016/j.electacta.2015.03.036
49. Wang G, Jin Z, Zhang M, Wang ZS. Self-Supporting AuCu@ Cu Elongated Pentagonal Bipyramids Toward Neutral Glucose Sensing. *Part Part Syst Charact.* 2016;33(10):771-8. doi:10.1002/ppsc.201600077
50. Fang B, Gu A, Wang G, Wang W, Feng Y, Zhang C, et al. Silver oxide nanowalls grown on Cu substrate as an enzymeless glucose sensor. *ACS Appl Mater Interfaces.* 2009;1(12):2829-34. doi:10.1021/am900576z